British Journal of Pharmacology

DOI:10.1111/j.1476-5381.2011.01705.x
www.brjpharmacol.org

RESEARCH PAPER

The metabolism and pharmacokinetics of phospho-sulindac (OXT-328) and the effect of difluoromethylornithine

G Xie[1], T Nie[1], GG Mackenzie[1], Y Sun[1], L Huang[1], N Ouyang[1], N Alston[1], C Zhu[1], OT Murray[1], PP Constantinides[2], L Kopelovich[3] and B Rigas[1]

[1]*Division of Cancer Prevention, Department of Medicine, Stony Brook University, Stony Brook, NY, USA,* [2]*Medicon Pharmaceuticals, Inc, Stony Brook, NY, USA, and* [3]*Division of Cancer Prevention, National Cancer Institute, Bethesda, MD, USA*

Correspondence
Basil Rigas, Division of Cancer Prevention, Stony Brook University, HSC, T17-080, Stony Brook, NY 11794-8173, USA.
E-mail: basil.rigas@stonybrook.edu

Keywords
metabolism; pharmacokinetics; phospho-sulindac; difluoromethylornithine; liver microsomes; gastrointestinal toxicity

Received
8 June 2011
Revised
9 August 2011
Accepted
7 September 2011

BACKGROUND AND PURPOSE

Phospho-sulindac (PS; OXT-328) prevents colon cancer in mice, especially when combined with difluoromethylornithine (DFMO). Here, we explored its metabolism and pharmacokinetics.

EXPERIMENTAL APPROACH

PS metabolism was studied in cultured cells, liver microsomes and cytosol, intestinal microsomes and in mice. Pharmacokinetics and biodistribution of PS were studied in mice.

KEY RESULTS

PS undergoes reduction and oxidation yielding PS sulphide and PS sulphone; is hydrolysed releasing sulindac, which generates sulindac sulphide (SSide) and sulindac sulphone (SSone), all of which are glucuronidated. Liver and intestinal microsomes metabolized PS extensively but cultured cells converted only 10% of it to PS sulphide and PS sulphone. In mice, oral PS is rapidly absorbed, metabolized and distributed to the blood and other tissues. PS survives only partially intact in blood; of its three major metabolites (sulindac, SSide and SSone), sulindac has the highest C_{max} and SSone the highest $t_{1/2}$; their AUC_{0-24h} are similar. Compared with conventional sulindac, PS generated more SSone but less SSide, which may contribute to the safety of PS. In the gastroduodenal wall of mice, 71% of PS was intact; sulindac, SSide and SSone together accounted for <30% of the total. This finding may explain the lack of gastrointestinal toxicity by PS. DFMO had no effect on PS metabolism but significantly reduced drug level in mouse plasma and other tissues.

CONCLUSIONS AND IMPLICATIONS

Our findings establish the metabolism of PS define its pharmacokinetics and biodistribution, describe its interactions with DFMO and largely explain its gastrointestinal safety.

Abbreviations

BNPP, bis(4-nitro-phenyl)-phosphate; DFMO, difluoromethylornithine; HLM, human liver microsome; PS, phospho-sulindac; RLC, rat liver cytosol; RLM, rat liver microsome; SSide, sulindac sulphide; SSone, sulindac sulphone; Trx, thioredoxin; UGT, UDP-glucuronosyltransferase

© 2011 The Authors
British Journal of Pharmacology © 2011 The British Pharmacological Society

Introduction

Inflammation is emerging as a pathophysiological mechanism that is central to seemingly disparate diseases, such as cardiovascular and rheumatologic disorders, cancer and neurodegenerative conditions, including Alzheimer's disease (Mantovani *et al.*, 2008). The appreciation of the unifying role of inflammation in human diseases has led to the evaluation of nonsteroidal anti-inflammatory drugs (NSAIDs) in their prevention (Cuzick *et al.*, 2009). For example, aspirin and sulindac prevent colon cancer in interventional human studies (Debinski *et al.*, 1995; DiSario *et al.*, 1997; Baron, 2009; Lanas and Ferrandez, 2009).

The application of NSAIDs to cancer prevention is hampered by two serious limitations: (i) their suboptimal efficacy, which is less than 50% (Kashfi and Rigas, 2005); and (ii) their side effects, which makes their long-term use problematic. For example, significant side effects are seen with sulindac, including gastrointestinal (up to 20% of the patients), CNS (up to 10%), skin rash and pruritus (5%), and transient elevations of hepatic enzymes in plasma (Roberts and Morrow, 2001). There have been two main responses to these limitations. First, several groups have tried to modify NSAIDs to enhance their efficacy and/or safety. Nitric oxide-donating NSAIDs and the amide derivative of sulindac represent two such approaches (Rigas, 2007; Rigas and Williams, 2008; Piazza *et al.*, 2009). Second, there have been efforts to develop combination strategies that include a conventional NSAID. The most successful combination includes sulindac and difluoromethylornithine (DFMO), which reduced by 69% the recurrence of adenomas in humans at risk for sporadic colon adenomas (Meyskens *et al.*, 2008). DFMO inhibits ornithine decarboxylase, which catalyses the rate-limiting step in polyamine synthesis, whereas sulindac stimulates polyamine acetylation and export from the cell. The end result is reduced intracellular polyamine levels leading to suppressed growth of cancer cells (Gerner and Meyskens, 2004; Gerner *et al.*, 2007).

Prompted by the efficacy of the sulindac/DFMO combination and by the considerable side effects of conventional sulindac, we synthesized phospho-sulindac (PS; OXT-328) in which a linker molecule bridges the conventional NSAID to the diethylphosphate moiety (Figure 1D). PS is more efficacious compared with conventional sulindac when used in both colon cancer prevention and treatment (Mackenzie *et al.*, 2010). In particular, in *Min* mice, a model of colon cancer in which mice develop numerous polyps in the small and large bowel, PS combined with DFMO prevented 90% of tumors (Mackenzie *et al.*, 2010). When evaluated as an anti-inflammatory agent in an arthritis model, PS demonstrated strong anti-inflammatory effects, essentially reversing joint inflammation and oedema (Huang *et al.*, 2011). The safety of PS has been documented in several preclinical models, including nude mice, *Min* mice and rats. When compared directly with conventional sulindac, the gastrointestinal toxicity of PS was similar to that of the vehicle control group (Mackenzie *et al.*, 2010).

Given the promising performance of PS against cancer and inflammation, its effective combination with DFMO, and its apparent safety, we studied its metabolism, pharmacokinetics (PK) and biodistribution in mice. In addition, we examined the effect of DFMO on the metabolism and pharmacokinetics of PS. Our results establish the metabolic pathways of PS *in vivo* and *in vitro*, its pharmacokinetics and biodistribution in mice, reveal a potentially important pharmacokinetic interaction with DFMO, and provide an explanation for its gastrointestinal safety.

Methods

Cell culture

SW480 and HT-29 colon cancer cells were grown as monolayers as recommended by ATTC. Cell growth was determined using the 3-(4,5-dimethylthiazol-2-yl)-2,5-diphenyltetrazolium bromide (MTT) assay (Promega, Madison, WI, USA) following the manufacturer's instructions.

HPLC analysis

The HPLC system consisted of a Waters Alliance 2695 Separations Module (Milford, MA, USA) equipped with a Waters 2998 photodiode array detector (328 nm) and a Thermo Hypersil BDS C18 column (150 × 4.6 mm, particle size 3 μm). The mobile phase consisted of a gradient between solvent A [formic acid, CH_3CN, H_2O (0.1:4.9:95 v/v/v)] and solvent B (CH_3CN) at a flow rate of 1 mL·min^{-1} at 30°C. We applied gradient elution from 30 to 100% solvent B from 0–6 min, and it was maintained at 100% solvent B until 8 min.

LC-MS/MS analysis

The LC-MS/MS system consisted of Thermo TSQ Quantum Access (Thermo-Fisher) triple quadrupole mass spectrometer interfaced by an electrospay ionization probe with an Ultimate 3000 HPLC system (Dionex Corporation, Sunnyvale, CA, USA). Chromatographic separations were achieved on a Luna C_{18} column (150 × 2 mm), and the mobile phase consisted of a gradient from 10 to 95% CH_3CN.

PS metabolism by liver and intestinal microsomes

PS was preincubated at 37°C for 5 min with a NADPH-regenerating solution (1.3 mM $NADP^+$, 3.3 mM D-glucose 6-phosphate, 3.3 mM $MgCl_2$ and 0.4 U·mL^{-1} glucose-6-phosphate dehydrogenase) in 0.1 M potassium phosphate buffer (pH 7.4). The reaction was initiated by the addition of liver microsomes (protein concentration 0.5 mg·mL^{-1}) or intestinal microsomes (protein concentration 0.25 mg·mL^{-1}) and samples were maintained at 37°C for various time periods. At the end of each of the incubations, 0.3 mL aliquots were mixed with 0.6 mL of CH_3CN, vortexed and then centrifuged for 10 min at 12 000× *g*, as described previously (Gao *et al.*, 2005). The supernatants were analysed by HPLC.

PS metabolism by rat and human liver cytosol

PS (100 μM) was preincubated at 37°C for 5 min with 10 mM dithiothreitol in 0.1 M Tris buffer (pH 7.4). The reaction was initiated by the addition of liver cytosol (protein concentration 2 mg·mL^{-1}) and samples were maintained at 37°C for

various time periods. At the end of each of the incubations, 0.3 mL aliquots were mixed with 0.6 mL of CH_3CN, vortexed and then centrifuged for 10 min at 12 000× *g*. The supernatants were analysed by HPLC.

PS metabolism by cultured human colon and breast cancer cells

To study the metabolism of PS, SW480 human colon cancer cells were seeded in 6-cm plates at a density of 10^5 cells·cm^{-2} in 4 mL of culture media and allowed to attach for 24 h. PS was added to the medium (final concentration 100 μM) and incubated with the cells for 6 h. The cells were subsequently washed three times with cold PBS and lysed using sonication. CH_3CN was added to extract PS and its metabolites from the cells, and the extracts were analysed by HPLC.

We also studied the metabolism of PS by MDA-MB-231 human breast cancer cells in which the expression of thioredoxin (Trx) was stably knocked down using interference RNA (short hairpin RNA).

Pharmacokinetic studies in mice

All animal care and experimental procedures were approved by the Institutional Animal Care and Use Committee at Stony Brook University. PS or sulindac was administered as a single treatment by gastric gavage to 5-week-old female BALB/C mice weighing approximately 20 g (Charles River Laboratories, Wilmington, MA, USA). Mice were killed at various time points after drug administration, and blood was collected and immediately centrifuged. The resulting plasma was deproteinized by immediately mixing it with a twofold volume of CH_3CN. PS and its metabolites were analysed by HPLC as described earlier.

Pharmacokinetic parameters in plasma were determined by non-compartmental pharmacokinetics data analysis using Pharmacokinetics Solutions 2.0 software (Summit Research Services, Montrose, CO, USA). The pharmacokinetic parameters determined include maximal plasma concentration (C_{max}), time to reach maximal plasma concentration (T_{max}), elimination half life ($t_{1/2}$) and the area under the concentration–time curve (AUC).

Tissue distribution study

At the times shown, the heart, liver and kidney of the mice given PS were collected, homogenized and sonicated in PBS. PS and its metabolites were extracted by adding a twofold volume of CH_3CN. After centrifugation for 10 min at 12 000× *g*, the supernatants were analysed by HPLC.

To determine the levels of PS and its metabolites in the wall of the stomach and duodenum, we harvested these two organs *in toto* after washing away their contents with PBS, three times and with 10% DMSO in PBS, twice, to remove gastric contents and PS that might be adsorbed on the gastroduodenal mucosa. Control experiments revealed that the 10% solution of DMSO did not damage the mucosa and removed, quantitatively, any adherent PS following its oral administration.

Statistical analyses

Results, obtained from at least three independent experiments, were expressed as mean ± SEM and analysed by one-way ANOVA followed by the Tukey test for multiple comparisons. $P < 0.05$ was considered statistically significant.

Results

PS metabolism by liver and intestinal microsomes

Our initial approach to the metabolism of PS was to determine its transformation by liver microsomes, which represent an enriched source of the major metabolic enzymes that, in general, render xenobiotic drugs more polar and, therefore, easier to eliminate from the body (Bajrami *et al.*, 2009). Such oxidative drug metabolism is the principal means of drug clearance.

As shown in Figure 1, the metabolism of PS by rat liver microsomes (RLMs) generates three metabolites, PS sulphone, sulindac (the parent compound) and SSone. Sulindac and SSone were identified by comparing their chromatographic retention time and UV spectra to those of authentic compounds. PS sulphone was identified by LC-MS/MS analysis. The mass spectrum of PS sulphone showed a $[M+Na]^+$ ion at m/z 602.8 (Figure 1B), which was further fragmented at its carboxyester and phosphotriester bonds to generate m/z 355 and 427 respectively (Figure 1C). This fragmentation pattern has also been observed for other phospho-NSAIDs such as phospho-ibuprofen (Xie *et al.*, 2011), indicating that the fragmentation at ester bonds is common for phospho-compounds. The identification of PS sulphone was also supported by its UV absorption spectrum that is identical to that of SSone; the linker-phosphate moiety of PS did not obviously contribute to its UV absorption. Likewise, PS and PS sulphide also have essentially the same UV spectrum as sulindac and SSide respectively (data not shown).

These findings, indicating oxidative and hydrolytic transformations of PS, suggest two metabolic pathways (Figure 1D). First, PS is oxidized to form PS sulphone, which can be then hydrolysed to produce SSone. Second, PS can be hydrolysed to produce sulindac, which can be then oxidized to produce SSone. Therefore, PS sulphone and sulindac are intermediate products in the metabolic transformations of PS by RLM, with SSone being the final product.

As shown in Figure 2A, the metabolism of PS by RLM was rather rapid. About 75% of PS was consumed within 10 min after the initiation of the reaction, and its conversion to metabolites was almost complete 40 min later, when only ~2% of PS remained in the reaction mixture. Consistent with this result, levels of SSone, the final product, steadily increased reaching a plateau at ~40 min. The two intermediate products, sulindac and PS sulphone, shared a similar kinetic behavior because both of these metabolites were produced from PS and both can be converted to SSone. The levels of sulindac and PS sulphone increased rapidly during the first 10 min of the reaction, indicating that initially the production of sulindac and PS sulphone from PS was dominant due to the high concentration of PS. With the PS level decreasing rapidly, the formation rate of sulindac and PS sulphone from PS decreased, leading to the steady decrease of the levels of sulindac and PS sulphone during the later phase of the reaction. Mouse liver microsomes gave results similar to those of RLM (data not shown).

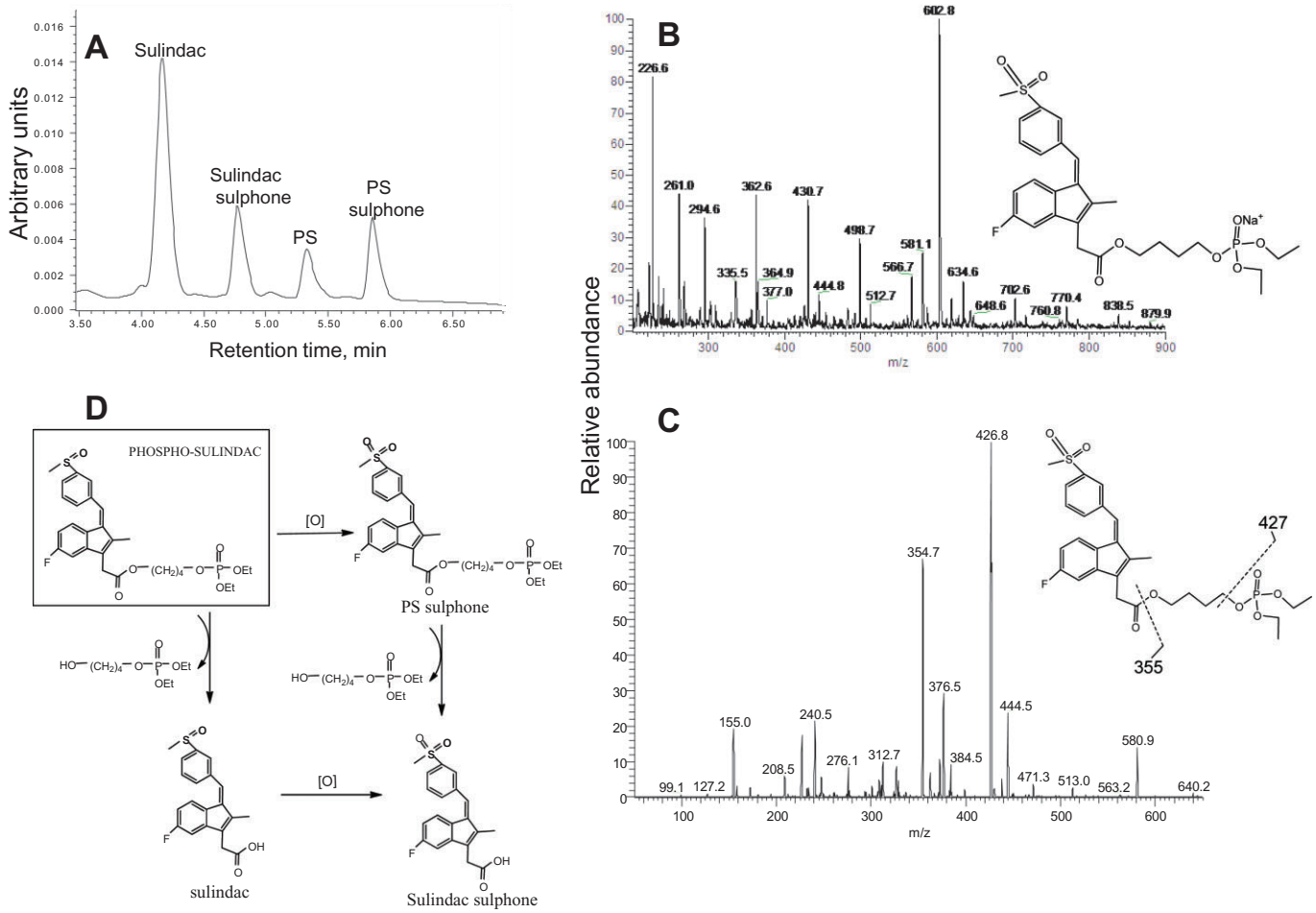

Figure 1

Metabolism of PS by rat and HLMs. (A) HPLC profile of PS and its metabolites generated by RLM 10 min after PS was incubated with RLM. PS and its metabolites were extracted and fractionated by HPLC. (B) MS spectrum of PS sulphone fraction collected from HPLC. (C) MS/MS spectrum of the major fragment ions of the PS sulphone ion. (D) Metabolic transformations of PS by liver microsomes.

As drug-metabolizing enzymes differ between species in isoform composition, expression and catalytic activity (Liu *et al.*, 2010), we next explored the metabolism of PS by human liver microsomes (HLMs). HLMs also converted PS to sulindac, PS sulphone and SSone (Figure 2B). The level of PS in the reaction mixture decreased continuously, whereas that of SSone increased steadily during the entire period of observation. On the other hand, the levels of sulindac and PS sulphone increased rapidly in the first 5 min and subsequently plateaued until the end of the observation period.

The metabolism of PS by HLM was qualitatively similar to that of RLM but differed from it in terms of the reaction rates (Figure 2). Compared with RLM, (i) PS is more stable in HLM; (ii) the elimination $t_{1/2}$ of PS in HLM is >3 times longer (38.8 min vs. 12.1 min); and (iii) the production of SSone is much slower in HLM (the final concentration of SSone is ~5 times lower). Thus, PS was more rapidly and more extensively metabolized by RLM than by HLM.

Given the gastrointestinal safety of PS, we also explored the metabolism of PS by human intestinal microsomes. PS generated sulindac, PS sulphone and SSone in intestinal microsomes showing the same metabolic changes as with liver microsomes. The level of PS in the reaction mixture decreased whereas the levels of the three metabolites increased during the entire period of observation (Supporting Information Figure S1).

Considering the structural features of PS and its products, we examined whether esterases are responsible for the hydrolysis of its carboxyester bond. This idea was supported by the fact that in rats the microsomal fraction contains ~70% of the total liver esterases, which are primarily carboxyesterases (CEs; Hayase and Tappel, 1969; Ljungquist and Augustinsson, 1971). PS (120 μM) was treated with porcine liver esterase (0.5 mg·mL^{-1}) at 37°C, and it was almost completely hydrolysed to release sulindac within 90 min after initiation of the reaction (Supporting Information Figure S2). Likewise, this esterase also hydrolysed PS sulphone and PS sulphide to release SSone and SSide respectively. These results established that the carboxyester bond of PS can be hydrolysed by esterases.

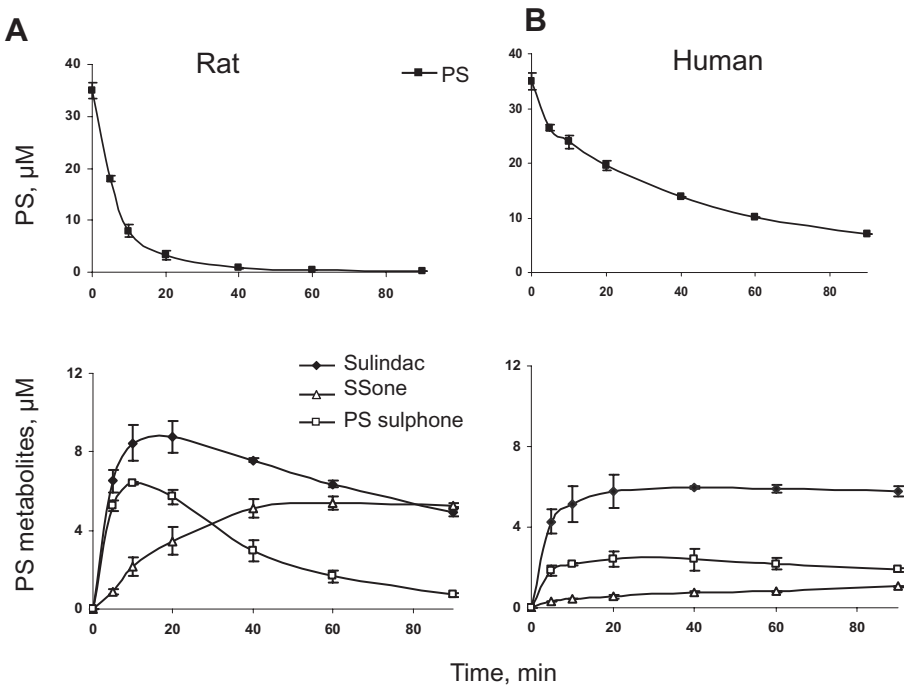

Figure 2

Kinetics of PS and its metabolites by rat and HLMs. PS (35 μM) was incubated with RLM (A) or HLM (B) at 37°C for up to 90 min. PS and its metabolites were extracted at the designated time points and assayed.

PS metabolism by liver cytosol

As conventional sulindac can be reduced to SSide by rat liver cytosol (RLC) (Ratnayake *et al.*, 1981), we examined the metabolism of PS by RLC. Three metabolites of PS (sulindac, PS sulphide and SSide) were readily detected in the reaction mixture of PS and RLC, indicating that PS undergoes hydrolysis and reduction reactions in RLC. PS can be hydrolysed and reduced to form sulindac and PS sulphide, respectively, both of which can further be transformed to SSide. The PS level in RLC decreased continuously, whereas that of SSide increased similarly during the entire period of observation (Figure 3). Sulindac and PS sulphide displayed similar kinetic patterns: both reached their peak value at ~2 h and subsequently became stable or slightly decreased until the end of the observation. Human liver cytosol generated similar results as RLC (data not shown).

PS metabolism by cultured cancer cells

Given the potency of PS to inhibit cancer cell growth (Mackenzie *et al.*, 2010), we studied its metabolism by cultured SW480 colon cancer cells. As shown in Figure 4, PS has ready access into the cells. Its levels plateaued within 10 min and primarily remained intact in the cells; sulindac, the hydrolysis product of PS, was undetectable. This finding is consistent with reports of low esterase activity in cells (Lamboursain *et al.*, 2002).

Although not hydrolysed, ~10% of PS was reduced and oxidized to form PS sulphide and PS sulphone, the two processes displaying somewhat different kinetics (Figure 4). PS sulphone reached its peak level within 10 min and then remained stable, whereas PS sulphide reached its peak level at about the same time but fell afterwards, probably because the reduction reaction of PS is reversible whereas the oxidation of PS is irreversible. Because the cells have low esterase activity and thus do not form appreciable amounts of sulindac, we did not detect any reduction/oxidation products of sulindac.

Thioredoxin (Trx) is known to be involved in the reduction of conventional sulindac to SSide (Anders *et al.*, 1981). To determine whether the reduction of PS is also Trx-dependent, we permanently knocked down the expression of Trx in human breast MDA-MB-231 cancer cells. Western blot analysis confirmed the elimination of Trx, and only 3% of Trx was still present in Trx-knockdown cells. We then treated the cells with PS (100 μM) for up to 6 h. At each time point, the level of PS sulphide in the Trx-knockdown cells was significantly lower than that in control cells, and the $AUC_{0\text{-}6h}$ decreased by 37% following Trx knockdown (Supporting Information Figure S3). These results indicate that Trx is involved in the reduction of PS, whereas other reductive enzymes such as methionine sulphoxide reductase A may be responsible for the remaining reductive enzyme activity in Trx-knockdown cells.

Metabolism and pharmacokinetics of PS in the mouse

We studied the pharmacokinetic properties of PS in mice, given a single dose of PS (158 $mg \cdot kg^{-1}$ in corn oil) by gastric gavage. Three major metabolites (sulindac, SSide and SSone) were detected by HPLC in plasma (Figure 5). Sulindac was the main metabolite of PS; its plasma C_{max} was 234 μM, the T_{max}

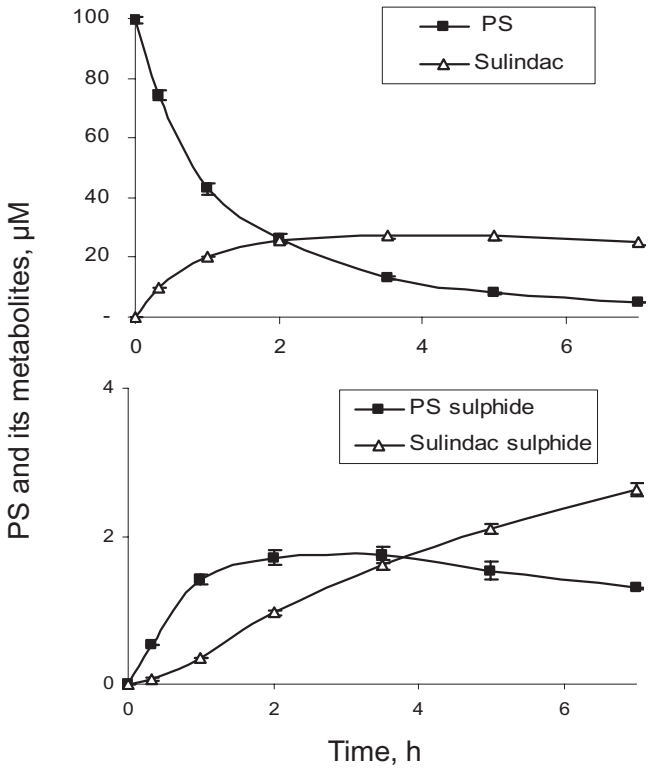

Figure 3

Metabolism of PS by RLC. Kinetics of PS and its metabolites by RLC. PS (100 µM) was incubated with RLC at 37°C for up to 7 h. PS and its metabolites were extracted at the designated time points and assayed.

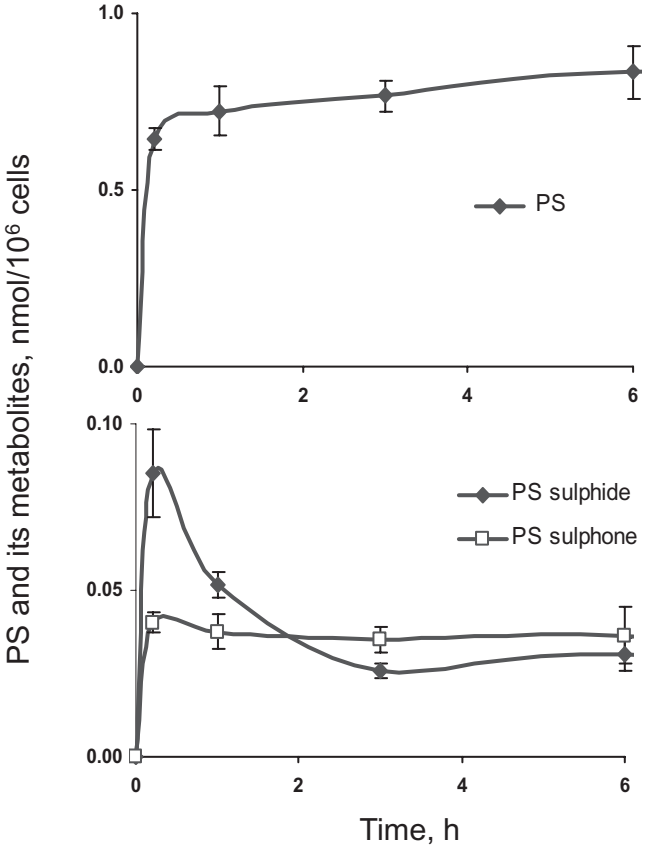

Figure 4

Kinetics of PS and its metabolites in SW480 cancer cells. PS (100 µM) was incubated with SW480 cells at 37°C for up to 6 h. PS and its metabolites were extracted at the designated time points and assayed.

was 2 h and the $t_{1/2}$ was 3.5 h. Emphasizing the rapid metabolic disposition of PS, plasma levels of sulindac dropped substantially by 4 h, becoming negligible at 8 h. SSone followed a similar pattern, but with much lower C_{max} and markedly prolonged $t_{1/2}$ (19.9 h). SSide appeared at even lower levels and with a broad peak.

Intact PS in murine plasma was not detectable by the UV detector, suggesting high carboxyesterase activity in blood. To test this idea, we evaluated the effect of bis(4-nitro phenyl)-phosphate (BNPP), a specific inhibitor for carboxyesterase (Morishita *et al.*, 2005), on the hydrolysis of PS by plasma *in vitro*. As shown in Supporting Information Figure S4, BNPP inhibited the hydrolysis of PS in a dose-dependent manner, and the carboxyesterase activity was completely blocked by the 10 mM concentration of BNPP. We then evaluated the effect of BNPP on the hydrolysis of PS *in vivo*. PS (158 mg·kg^{-1} in corn oil) generated 2.9 µM intact PS in mouse blood 1 h following its co-administration with BNPP (200 mg·kg^{-1}), whereas intact PS was not detected in the blood of mice not receiving BNPP. Thus, BNPP effectively inhibits the hydrolysis of PS *in vitro* and *in vivo*.

For purposes of comparison, we performed parallel pharmacokinetic studies of conventional sulindac administered to mice orally at a dose equimolar to PS (100 mg·kg^{-1} in corn oil). In addition to intact sulindac, we detected in plasma its two main metabolites, SSide and SSone; their $AUC_{0\text{-}24h}$ were SSide >> sulindac >> SSone. As shown in Table 1, there are four main pharmacokinetic differences between PS and conventional sulindac. First, in terms of $AUC_{0\text{-}24h}$ the three main metabolites of PS have similar $AUC_{0\text{-}24h}$ values (632–707 µM*h), whereas those of conventional sulindac vary widely (357–2697 µM*h). Second, the pharmacokinetic parameters of SSone derived from PS differ from those of SSone derived from conventional sulindac: T_{max}: 2 versus 24 h; $t_{1/2}$: 19.9 versus 3.2 h; $AUC_{0\text{-}24h}$: 673 versus 357 µM*h. And, third, even though the doses of the PS and sulindac were equimolar, the sum of the plasma $AUC_{0\text{-}24h}$ of the three compounds (sulindac, SSone and SSide) derived from PS is 44% of the $AUC_{0\text{-}24h}$ of the same three compounds derived from conventional sulindac.

We also determined the pharmacokinetic parameters of PS administered at the same dose either orally dissolved in 0.5% carboxymethyl cellulose or intraperitoneally dissolved in PBS (from a stock in DMSO) (Figure 6 and Table 1). Compared with the values of PS administered orally in corn oil, in both cases, the C_{max} of each compound was significantly lower; the $t_{1/2}$ was similar with the exception of SSone that was reduced by about 75%; and the total $AUC_{0\text{-}24h}$ (sulindac, SSone, SSide) was reduced by 80–90%.

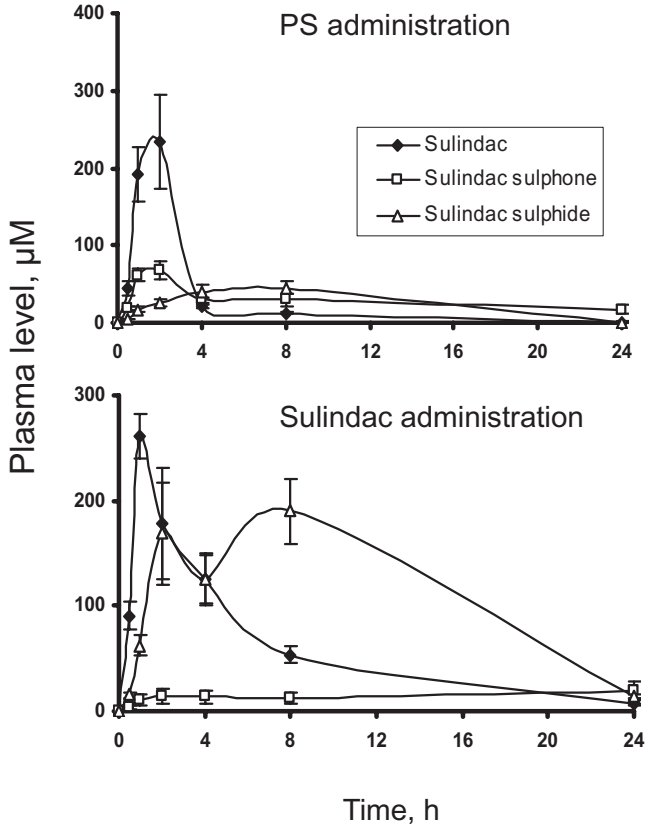

Figure 5

Comparison of the pharmacokinetics of PS and sulindac in mice. Equimolar doses of sulindac (100 mg·kg^{-1}) and PS (158 mg·kg^{-1}) in corn oil were administered to mice as a single dose by gastric gavage. Plasma levels of PS metabolites were determined at the times shown.

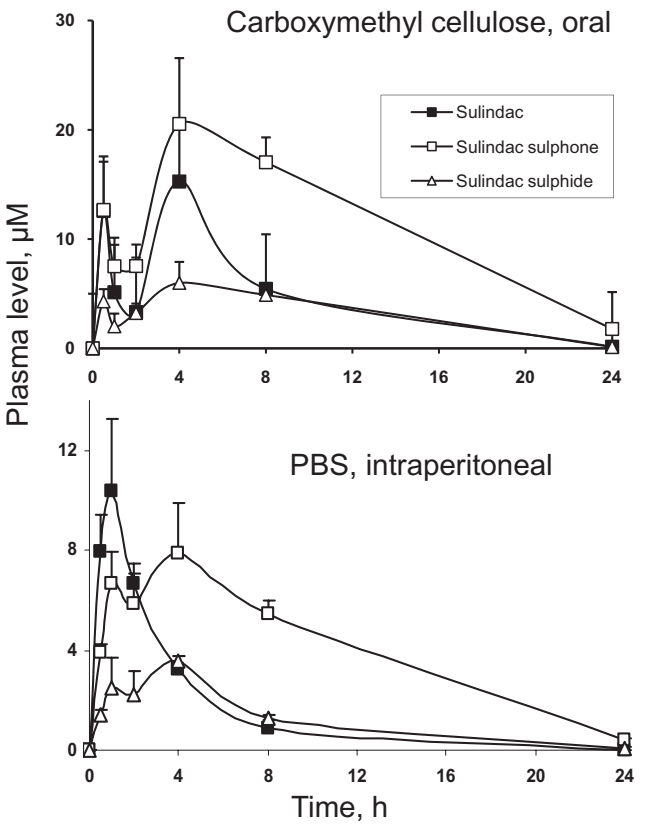

Figure 6

The pharmacokinetics of PS administered in carboxymethyl cellulose or PBS to mice. PS (150 mg·kg^{-1}) was administered to mice as a single dose orally in carboxymethyl cellulose (upper graph) or i.p. in PBS (lower graph). Plasma levels of PS metabolites were determined at the times shown.

Tissue distribution of PS in mice

To evaluate the biodistribution of PS in mice, we determined the drug levels in heart, liver and kidney. In addition to the three major metabolites that we detected in plasma, we also detected intact PS and PS sulphone in these tissues (Table 2). It is evident that, despite its rapid hydrolysis in blood, PS survives in appreciable amounts in other tissues, with the liver showing the highest level of PS.

The simplest explanation of our findings was that at the dose of 150 mg·kg^{-1}, PS plasma levels are below our detection limit. Consequently, a dose of PS three times higher (450 mg·kg^{-1}) was administered to mice. As expected, appreciable amounts of intact PS and PS sulphone were detected in plasma (Table 2), confirming that PS can survive in blood, which transports it to various tissues. In addition, three glucuronidation metabolites of PS (sulindac glucuronide, SSone glucuronide and SSide glucuronide) were detected in liver; whereas their levels in plasma and other tissues are quite low (Table 2). SSone glucuronide and SSide glucuronide were identified by LC-MS/MS analysis. The mass spectrum of SSone glucuronide showed a [M-H]$^-$ ion at m/z 547, which was fragmented at its acyl-glucuronide bond to generate m/z 326.8 and 192.7 (Supporting Information Figure S5A). Likewise, the mass spectrum of SSide glucuronide showed a [M-H]$^-$ ion at m/z 515, which was also fragmented at its glucuronide bond to produce m/z 294.5 and 193 (Supporting Information Figure S5B). This fragmentation pattern was also observed for other glucuronides such as indomethacin glucuronide, indicating that the fragmentation at their glucuronide bonds is common for acyl glucuronides. The identification of SSone glucuronide and SSide glucuronide were also confirmed using authentic compounds. SSide glucuronide was detected in abundance (704 μM) in bile obtained from the gallbladder of mice 4 h after the oral administration of PS (500 mg·kg^{-1}).

Given the superior gastrointestinal safety of PS over conventional sulindac (Mackenzie *et al.*, 2010; Huang *et al.*, 2011), we determined the $AUC_{0\text{-}24h}$ of drug levels in the gastroduodenal wall of mice following oral administration of equimolar amounts of PS or sulindac. As expected, the equimolar doses of PS and sulindac generated similar total drug levels (Table 3). Unlike other organs (Table 2), however, 71% of PS was intact, sulindac was its major metabolite, and SSide and SSone were present at very low levels. Conventional sulindac remained largely intact (66%) and SSide was its main metabolite (29% of the total mass), whereas SSone represented only 5% of the total. Compared with mice treated with an equimolar amount of conventional sulindac,

Table 1

Pharmacokinetic parameters of phospho-sulindac and sulindac at equimolar doses in mice

Drug administered	Delivery vehicle	Delivery route	Metabolite measured	C_{max} (μM)	T_{max} (h)	Elimination $t_{1/2}$ (h)	AUC (μM*h)	Sum of AUC (μM*h)
Phospho-sulindac	Corn oil	Oral	Sulindac	234	2.0	3.5	707	2012
			SSone	69	2.0	19.9	673	
			SSide	45	8.0	2.9	632	
	Carboxymethyl cellulose	Oral	Sulindac	15	4.0	3.1	117	462
			SSone	21	4.0	4.9	269	
			SSide	6	4.0	3.0	76	
	PBS	IP	Sulindac	11	0.8	5.2	41	168
			SSone	8	4.0	4.1	97	
			SSide	4	4.0	4.2	30	
Sulindac	Corn oil	Oral	Sulindac	261	1.0	5.4	1476	4530
			SSone	20	24.0	3.2	357	
			SSide	190	8.0	4.3	2697	

Experiments were done at least twice; values were generally within 10%.
Mice were given 158 mg·kg^{-1} phosphosulindac or 100 mg·kg^{-1} sulindac.

Table 2

Drug levels in mouse tissues following oral administration of PS at 150 and 450 mg·kg^{-1}

	Intact PS pmol·mg^{-1} protein	PS sulphone	Sulindac (mean ± SEM)	SSide	SSone	Sulindac glucuronide	SSone glucuronide	SSide glucuronide
Dose = 150 mg·kg^{-1}								
Liver	39 ± 17	18 ± 8	204 ± 49	19 ± 2	79 ± 42	15 ± 4	13 ± 3	25 ± 12
Heart	5 ± 1	1 ± 1	152 ± 34	12 ± 3	39 ± 7	2 ± 0	3 ± 0	1 ± 0
Kidney	4 ± 1	3 ± 1	499 ± 105	25 ± 7	94 ± 18	2 ± 1	3 ± 1	2 ± 0
*Plasma	ND	ND	64 ± 10	5 ± 1	14 ± 2	1 ± 0	1 ± 0	1 ± 0
Dose = 450 mg·kg^{-1}								
Liver	52 ± 8	17 ± 6	372 ± 40	21 ± 6	84 ± 40	66 ± 11	14 ± 2	17 ± 4
Heart	31 ± 6	8 ± 1	538 ± 63	19 ± 4	99 ± 27	22 ± 6	15 ± 4	4 ± 2
Kidney	14 ± 3	6 ± 1	888 ± 107	25 ± 8	136 ± 66	52 ± 15	10 ± 2	7 ± 2
*Plasma	5 ± 1	1 ± 0	157 ± 2	6 ± 2	26 ± 8	8 ± 2	4 ± 1	1 ± 0

*Plasma levels were expressed as μM.
ND, not detectable.

in mice treated with PS, (i) the amount of sulindac was 3.0 times lower; (ii) the amount of SSide was 9.4 times lower; and (iii) SSone was 1.8 times lower. These striking differences between the two compounds may account for their differences in gastroduodenal toxicity.

The effect of DFMO on the metabolism, pharmacokinetics and tissue distribution of PS

The combination of PS with DFMO was much more effective in preventing colon cancer efficacy in *Min* mice than PS alone (Mackenzie *et al.*, 2010). As already mentioned, there is a biochemical rationale for the enhanced efficacy of this combination. Nevertheless, the possibility exists that DFMO may enhance the efficacy of PS by changing its metabolism and/or pharmacokinetic properties, especially as DFMO can induce intestinal villous atrophy and fluid loss, which may influence the intestinal absorption of PS (Yarrington *et al.*, 1983).

Initially, we examined the effect of DFMO on the metabolism of PS by HLM. As shown in Figure 7A, both the metabolism and the metabolic kinetic profiles of PS and its metabolites (sulindac, PS sulphone and SSone) are virtually

Table 3

Gastroduodenal drug levels in mice treated with PS or sulindac

	PS AUC_{0-24h} in stomach-duodenum pmol·mg^{-1} protein*h	% of total	Sulindac pmol·mg^{-1} protein*h	% of total
PS	16 698	71	0	0
PS sulphone	94	0	0	0
Sulindac	5 551	23	16 465	66
SSide	774	3	7 298	29
SSone	567	2	1 037	4
Total	23 684	100	24 800	100

PS 150 mg·kg^{-1} or sulindac 100 mg·kg^{-1} (equimolar) in corn oil were given orally once.
Samples were obtained at 0, 1, 2, 4, 8, 12 and 24 h post-dosing.
Values are the average of two mice; results from each pair were within 15%.

Table 4

Effect of DFMO on biodistribution of PS and its metabolites to mouse tissues

	Drug administration	Sulindac AUC_{0-4h}, pmol·mg^{-1} protein*h	SSone	SSide	PS	PS sulphone	Total	% of control
*Plasma	PS	227 ± 4	137 ± 1	88 ± 7	ND	ND	451 ± 2	
	PS + DFMO	126 ± 3	99 ± 4	64 ± 11	ND	ND	296 ± 19	66%
Liver	PS	716 ± 14	415 ± 6	211 ± 4	56 ± 3	74 ± 8	1471 ± 25	
	PS + DFMO	432 ± 20	317 ± 14	134 ± 5	73 ± 2	61 ± 6	1018 ± 37	69%
Heart	PS	263 ± 49	162 ± 23	199 ± 24	21 ± 3	33 ± 4	679 ± 104	
	PS + DFMO	122 ± 11	98 ± 2	137 ± 21	14 ± 1	8 ± 1	379 ± 13	56%
Kidney	PS	740 ± 108	364 ± 34	304 ± 31	10 ± 3	19 ± 3	1437 ± 179	
	PS + DFMO	514 ± 25	309 ± 21	241 ± 29	7 ± 2	14 ± 3	1085 ± 79	75%

*Metabolite levels in the plasma were expressed as μM*h in plasma.
ND, not detectable.

identical in the absence or presence of DFMO. Rat and mouse liver microsomes gave similar results (not shown). Likewise, DFMO had no effect on the metabolism of PS by human intestinal microsomes (not shown).

To evaluate the effect of DFMO on the pharmacokinetics of PS in mice, DFMO (2% in their drinking water) was given to mice for 2 days before the administration of a single dose of PS (150 mg·kg^{-1} in corn oil). Following DFMO treatment, the plasma levels of sulindac, SSide and SSone, were significantly decreased at 1 and 2 h, becoming the same at 4h (Figure 7B). Consequently, DFMO decreased the AUC_{0-4h} of sulindac, SSone and SSide in plasma by 45%, 28% and 27%, respectively, compared with controls. Similar to blood, DFMO treatment decreased the 1 h and 2 h levels of the three PS metabolites in mouse liver, heart and kidney. PS and PS sulphone were also detected at low levels in these organs, and DFMO treatment decreased their levels in mouse hearts and kidneys. These results are shown in Figure 7C as the cumulative the 1 and 2 h levels of the 'total metabolites' (the sum of sulindac, SSide and SSone). Table 4 shows that in every case the AUC_{0-4h} of each metabolite in plasma, liver, heart and kidney was decreased following DFMO treatment. Furthermore, the cumulative AUC of the 'total PS metabolites' was decreased by DFMO in plasma, liver, heart and kidney by 34, 31, 44 and 25% respectively. These results indicate that DFMO, although not influencing PS metabolism, inhibits PS absorption into blood after oral administration and its biodistribution to other tissues.

Discussion and conclusions

Our results have established the metabolic pathways of PS *in vitro* and *in vivo* and determined its pharmacokinetic parameters and tissue distribution in mice. They also demonstrate that although DFMO did not affect the metabolism of PS, it

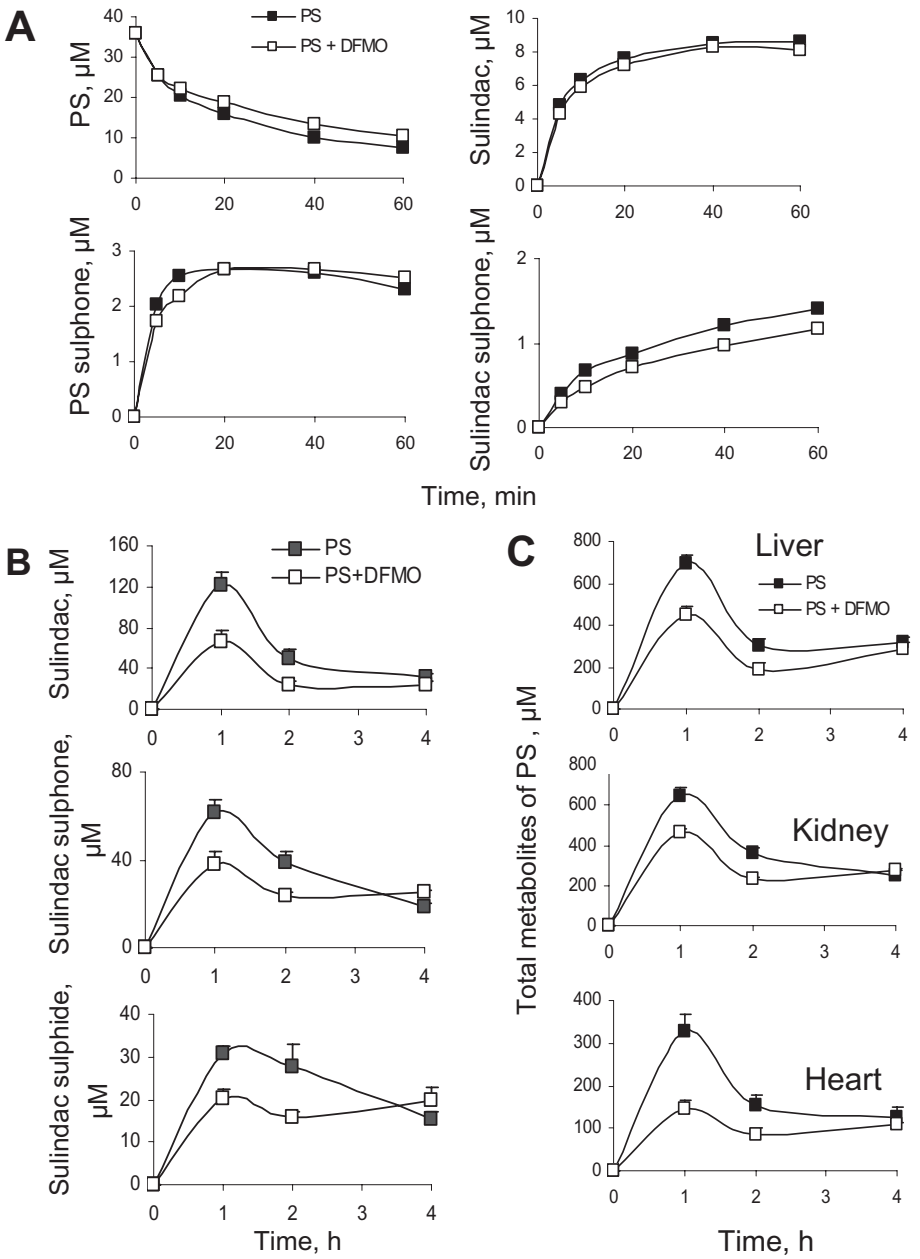

Figure 7

Effect of DFMO on the metabolism, pharmacokinetics and tissue distribution of PS. (A) PS (35 μM) was incubated with HLM for up to 60 min in the absence or presence of 5 mM DFMO. PS and its metabolites were extracted at the indicated time points and assayed. (B) Study mice were given water with or without 2% DFMO for 2 days. Following that, a single dose of PS 200 mg·kg^{-1} was administered by gastric gavage, and plasma levels of PS metabolites were measured. (C) The livers, kidneys and hearts of the mice studied in Panel B were harvested, and the PS metabolites were measured. Data were expressed as the sum of the levels of PS and its metabolites in each tissue.

did interfere with its pharmacokinetics and biodistribution. The latter is important, given the synergy between PS and DFMO in colon cancer prevention (Mackenzie *et al.*, 2010), which mirrors the strong prevention of sporadic colon polyps by conventional sulindac plus DFMO (Meyskens *et al.*, 2008).

The metabolism of PS (Figure 8), established through a series of studies that included liver microsomes and cytosols, cultured cells and mice, follows four metabolic pathways:

- *Oxidation/reduction reactions* – PS can be reduced and oxidized to form PS sulphide and PS sulphone respectively.
- *Hydrolysis reactions* – PS can be hydrolysed to produce sulindac; PS sulphide can be hydrolysed to SSide; and PS sulphone can be hydrolysed to SSone. PS, PS sulphide and PS sulphone could theoretically be hydrolysed to release their diethylphosphate moiety generating the respective alcohols, but we were unable to isolate such products.

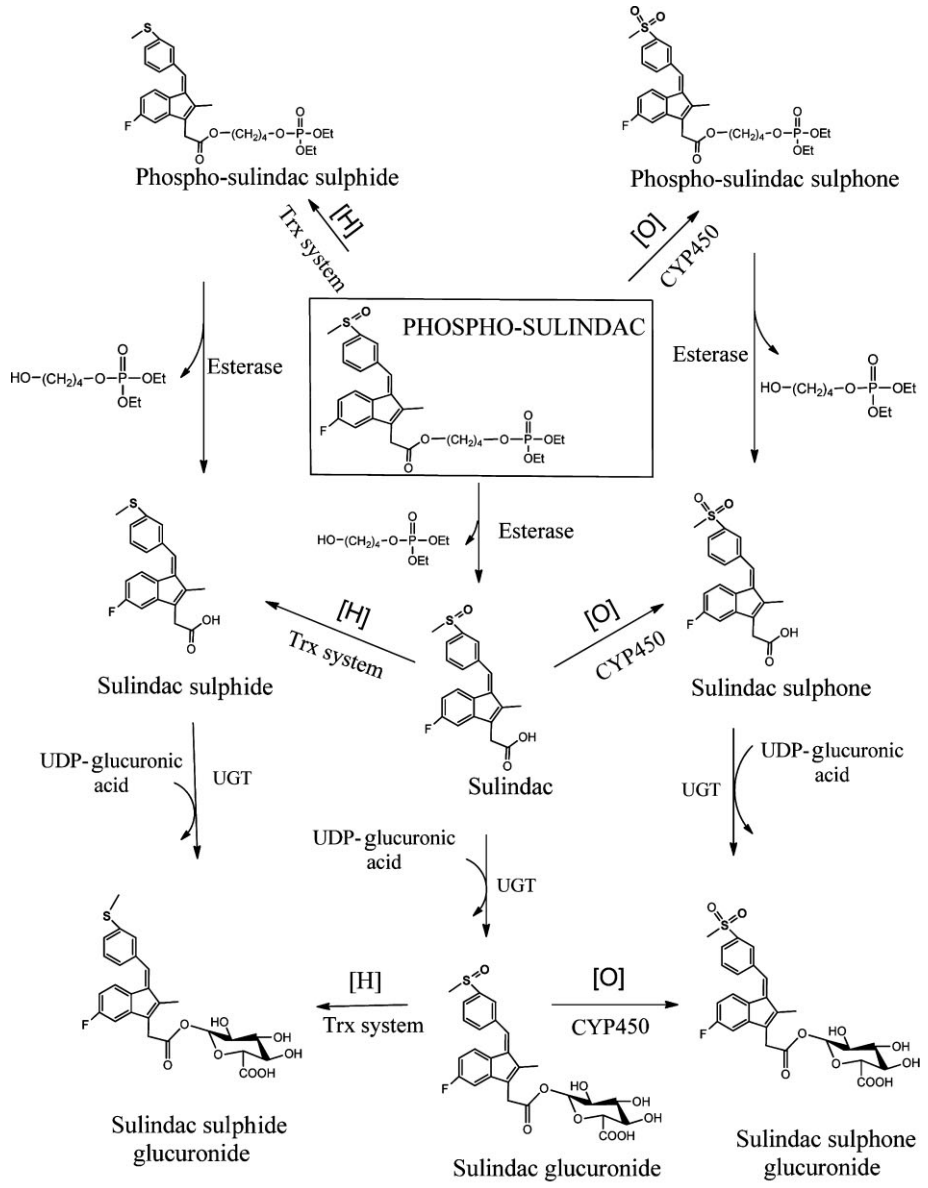

Figure 8

Overall metabolic pathways of PS *in vitro* and *in vivo*. PS is subjected to a series of reduction/oxidation reactions of its sulphoxide group and/or hydrolytic cleavages of its carboxy ester bond. The end result is eight metabolic products through three distinct and ultimately converging pathways.

- *Transformations of sulindac* – Sulindac, a metabolite of PS, can follow the known metabolism of conventional sulindac, which includes its oxidation or reduction to SSone and SSide respectively (Davis and Guenthner, 1985).
- *Glucuronidation reactions* – Sulindac, SSone and SSide undergo conjugation to glucuronic acid at their – COOH groups forming glucuronides. Thus the metabolically most active parts of PS are its sulphoxide moiety and its carboxyester bond.

At least three enzymes appear to play important roles in these transformations of PS: Trx, carboxyesterases and UDP-glucuronosyltransferases (UGTs). The mechanistic hallmark of Trx is the two vicinal thiols at its active site that carry out most of its enzymatic activity (Kaimul *et al.*, 2007). Trx catalyses part of the reduction of PS to PS sulphide; when its expression was knocked down, the reduction of PS was substantially decreased. Based on Trx's known mechanism of action, it is reasonable to assume that in this process Trx becomes oxidized (its two -SH groups form a disulphide) and is restored to its original state by Trx reductase (Kaimul *et al.*, 2007). Conventional sulindac is also reduced by Trx (Anders *et al.*, 1981). As the kinetics of PS metabolism in cultured cells

suggest, the reduction of PS is reversible and its oxidation irreversible, both similar to those of sulindac (Davis and Guenthner, 1985; Hamman *et al.*, 2000).

Carboxyesterases participate in the hydrolysis of PS, an ester drug. This idea was supported by our finding that BNPP, a specific inhibitor for carboxyesterases, can completely inhibit the hydrolysis of PS. Carboxyesterases are abundant in mouse small intestine, plasma and liver microsomes (Taketani *et al.*, 2007), and are likely to account for the significant hydrolysis of PS in mice. Based on their substrate specificities, carboxyesterases are primarily classified into carboxyesterases-1, which hydrolyse esters with a large acyl moiety, and carboxyesterases-2, which hydrolyse those with a small acyl group (Taketani *et al.*, 2007; Hosokawa, 2008). PS has a much larger acyl group than the substrates for carboxyesterases-1 such as cocaine, meperidine, methylphenidate and oseltamivir (Hosokawa, 2008), suggesting that PS may be a substrate for carboxyesterases-1.

Glucuronidation is one of the major pathways that eliminate and detoxify lipophilic xenobiotics. UGTs glucuronidate three metabolites of PS (sulindac, SSone or SSide) at their –COOH group to form the corresponding acyl-glucuronides. Thus it was not surprising to find that their levels in bile approached mM concentrations, whereas in blood they were at the μM level, indicating that the bile is a major excretion route for PS. Acyl glucuronides are known to be susceptible to intramolecular acyl migration and to show high electrophilicity in reactions with sulphanyl and hydroxyl groups of proteins (Kirschning *et al.*, 1997). These two properties of the acyl glucuronides may explain, in part, their low blood levels.

Mouse, rat and HLMs generated the same metabolites of PS, suggesting the same metabolic pathway of PS in these species. This finding, reflecting the highly conserved drug-metabolizing enzymes among different species, helps to predict the efficacy of PS in humans, as its metabolites appear important for its anticancer effect. On the other hand, PS was metabolized more extensively and rapidly by the liver microsomes of mouse and rat than of human. These *in vitro* kinetic data, correlated with our pharmacokinetic data in mice, could help predict its pharmacokinetics in humans (Liu *et al.*, 2010).

The pharmacokinetic and biodistribution studies demonstrated that following its administration to mice, PS is rapidly absorbed, metabolized and distributed to blood and other tissues. Our pharmacokinetic findings provide important information concerning several aspects of the pharmacology of PS, including its administration, efficacy and safety, as discussed below.

It is clear from our data that corn oil is better than carboxymethyl cellulose and PBS for the administration of PS, overcoming its poor aqueous solubility, which hinders efficiency and bioavailability (Gupta and Moulik, 2008). Corn oil is known to form microemulsions, which enhance the bioavailability of hydrophobic drugs by increasing their solubility and residence time in the intestine through bioadhesion (Acosta *et al.*, 2004).

The pharmacokinetic study showed that PS undergoes rapid hydrolysis in mice, which nonetheless is not complete, allowing its transport to other tissues where it is present at variable but always low levels (except for the gastroduodenal wall). Given that PS inhibits cancer cell growth ≥13-fold more potently than sulindac (Mackenzie *et al.*, 2010), its presence in tissues may be critical to its anticancer efficacy. In addition to intact PS, four of its metabolites, which are present at substantial concentrations, are known to have anticancer potency. Sulindac and SSide inhibit cancer cell growth through a multitude of mechanisms, both COX-dependent and COX-independent (Shiff *et al.*, 1995; Hanif *et al.*, 1996; Shiff and Rigas, 1999). PS sulphide inhibits the growth of human colon cancer cells more potently than PS by reducing the intracellular polyamine pool that is essential for cancer cell growth (Huang *et al.*, 2010). Finally, SSone inhibits cancer growth by stimulating polyamine acetylation and export from the cell (Babbar *et al.*, 2003).

These pharmacokinetic data indicate that PS behaves both as a primary anticancer agent and as a pro-drug. Lowering exposure of PS to carboxyesterases may enhance its anticancer efficacy. Of great interest, human plasma has ~10-fold lower carboxyesterase activity compared with mice (Nagy *et al.*, 2000). Thus, it is reasonable to predict that in humans the plasma and tissue levels of intact PS will be higher, leading to greater anticancer efficacy. The role of esterases in the efficacy of PS is emphasized by our finding that cultured human cancer cells and a normal colon cell line lack detectable esterase activity. Thus, PS is not hydrolysed by these cells, a finding consistent with its higher potency compared with its hydrolysis products (Mackenzie *et al.*, 2010).

The pharmacokinetic comparison between PS and conventional sulindac yielded results that were likely to explain the greater safety of PS, particularly concerning gastroduodenal toxicity, the most frequent side effect of sulindac. A striking feature of the pharmacokinetics of PS versus sulindac was that equimolar concentrations of these two compounds generated very different amounts of blood metabolites: the $AUC_{0\text{–}24h}$ of the 'total metabolites' (sulindac, SSide and SSone) in plasma following PS administration is ~2.3-fold lower than that obtained with sulindac administered at an equimolar dose. Furthermore, in terms of individual metabolites, PS generated roughly half the amount of sulindac, one-fourth the amount of SSide, and twice the amount of SSone in plasma based on $AUC_{0\text{–}24h}$ values. These are very favourable differences in terms of safety. SSone has a better safety profile than SSide, in particular regarding gastrointestinal toxicity (Glavin and Sitar, 1986). The underlying mechanisms have been investigated extensively; for example, SSide inhibits COX-1 and COX-2 >48-fold more potently than SSone, depleting the physiologically important prostaglandins (PGs) and contributing to the higher toxicity of SSide (Piazza *et al.*, 2009). Likewise, SSide, but not SSone, inhibits 5-lipoxygenase, suppressing production of leukotrienes, important immune mediators similar to PGs (Steinbrink *et al.*, 2010). Moreover, SSide, but not SSone, causes mitochondria uncoupling that induces hepatic toxicity (Leite *et al.*, 2006).

Given the importance of gastroduodenal safety for NSAIDs in general and the apparent safety of PS (Mackenzie *et al.*, 2010), we focused further on the biodistribution of PS in the stomach and duodenum and compared it with that of an equimolar dose of sulindac. The equally striking difference between the two concerned: (i) the presence of predominantly intact PS (71% of the total); and (ii) the consequently drastically reduced levels of sulindac (1/3), SSide (1/9) and

SSone (1/2). These differences center around their potential effects on PG synthesis and epithelial cell survival, two critical determinants of gastric mucosal integrity, that is, of the propensity to develop erosions and ulcers (Wallace and Vong, 2008). NSAIDs damage the gastric epithelium through several mechanisms, including direct killing of epithelial cells, particularly by acidic NSAIDs, but most importantly through their systemic ability to suppress PG synthesis (Wallace, 2008).

In this regard, PS has two important advantages over conventional sulindac. First, PS does not inhibit PG synthesis, as shown both in cultured cells and in *Min* mice; the levels of PGE_2 in the intestinal mucosa and of its metabolite 13,14-dihydro-15-keto PGE_2 in blood did not change in response to PS (Mackenzie *et al.*, 2010). Sulindac, in contrast, is a COX inhibitor, blocking PG synthesis. Second, while sulindac is acidic, PS is not; acidic NSAIDs migrate easily into surface epithelial cells, inducing mucosal injury (Sostres *et al.*, 2010).

Finally, of particular interest was the interaction between DFMO and PS, especially in view of the potential role of PS in colon cancer prevention, for which it may be combined with DFMO (Mackenzie *et al.*, 2010; 2011). DFMO did not influence the metabolism of PS by liver microsomes. DFMO, however, reduced drug levels in mouse blood and other tissues. DFMO has been reported to induce intestinal changes such as villous atrophy of the mucosa and fluid loss (Yarrington *et al.*, 1983). Such an effect is likely to reduce PS absorption into blood through the intestinal mucosa and may explain our finding. The reduced drug bioavailability by DFMO may affect drug efficacy, which could be addressed by optimizing the dosing regimen. Importantly, we recently showed that in combination with DFMO, PS reduced the number of intestinal tumors in *Min* mice by 90%, and this combination produced no significant side effects in mice (Mackenzie *et al.*, 2010).

In conclusion, our work shows that PS undergoes extensive transformations *in vivo* and *in vitro* yielding at least eight metabolites. These metabolites, together with the intact PS, may play important roles in cancer control. The pharmacokinetic and biodistribution features of PS provide a likely explanation of its greater safety, especially regarding its ability to spare the gastroduodenal mucosa.

Acknowledgements

This work was supported by the National Institute of Health Grants R01-CA139453, N01-CN-43302 WA#7, RCA153662A and HHSN261201000109C. This research was also supported in part by the Intramural Research Program of the National Cancer Institute. We thank R. Rieger and T. Koller, Stony Brook University, for the expert LC-MS/MS analysis of our samples and the shared instrumentation grant, NIH/NCRR 1 S10 RR023680-1.

Conflicts of interest

The authors have nothing to disclose except for B.R., who has an equity position in Medicon Pharmaceuticals, Inc.

References

Acosta EJ, Harwell JH, Sabatini DA (2004). Self-assembly in linker-modified microemulsions. J Colloid Interface Sci 274: 652–664.

Anders MW, Ratnayake JH, Hanna PE, Fuchs JA (1981). Thioredoxin-dependent sulfoxide reduction by rat renal cytosol. Drug Metab Dispos 9: 307–310.

Babbar N, Ignatenko NA, Casero RA Jr, Gerner EW (2003). Cyclooxygenase-independent induction of apoptosis by sulindac sulfone is mediated by polyamines in colon cancer. J Biol Chem 278: 47762–47775.

Bajrami B, Zhao L, Schenkman JB, Rusling JF (2009). Rapid LC-MS drug metabolite profiling using microsomal enzyme bioreactors in a parallel processing format. Anal Chem 81: 9921–9929.

Baron JA (2009). Aspirin and NSAIDs for the prevention of colorectal cancer. Recent Results Cancer Res 181: 223–229.

Cuzick J, Otto F, Baron JA, Brown PH, Burn J, Greenwald P *et al.* (2009). Aspirin and non-steroidal anti-inflammatory drugs for cancer prevention: an international consensus statement. Lancet Oncol 10: 501–507.

Davis PJ, Guenthner LE (1985). Sulindac oxidation/reduction by microbial cultures; microbial models of mammalian metabolism. Xenobiotica 15: 845–857.

Debinski HS, Trojan J, Nugent KP, Spigelman AD, Phillips RKS (1995). Effect of sulindac on small polyps in familial adenomatous polyposis. Lancet 345: 855–856.

DiSario JA, Alberts DS, Tietze CC, Khullar SK, Bohman VD, Larsen BR *et al.* (1997). Sulindac induces regression and prevents progression of sporadic colorectal adenomas. Gastroenterology 112: A555.

Gao J, Kashfi K, Rigas B (2005). *In vitro* metabolism of nitric oxide-donating aspirin: the effect of positional isomerism. J Pharmacol Exp Ther 312: 989–997.

Gerner EW, Meyskens FL Jr (2004). Polyamines and cancer: old molecules, new understanding. Nat Rev Cancer 4: 781–792.

Gerner EW, Meyskens FL Jr, Goldschmid S, Lance P, Pelot D (2007). Rationale for, and design of, a clinical trial targeting polyamine metabolism for colon cancer chemoprevention. Amino Acids 33: 189–195.

Glavin GB, Sitar DS (1986). The effects of sulindac and its metabolites on acute stress-induced gastric ulcers in rats. Toxicol Appl Pharmacol 83: 386–389.

Gupta S, Moulik SP (2008). Biocompatible microemulsions and their prospective uses in drug delivery. J Pharm Sci 97: 22–45.

Hamman MA, Haehner-Daniels BD, Wrighton SA, Rettie AE, Hall SD (2000). Stereoselective sulfoxidation of sulindac sulfide by flavin-containing monooxygenases. Comparison of human liver and kidney microsomes and mammalian enzymes. Biochem Pharmacol 60: 7–17.

Hanif R, Pittas A, Feng Y, Koutsos MI, Qiao L, Staiano-Coico L *et al.* (1996). Effects of nonsteroidal anti-inflammatory drugs on proliferation and on induction of apoptosis in colon cancer cells by a prostaglandin-independent pathway. Biochem Pharmacol 52: 237–245.

Hayase K, Tappel AL (1969). Microsomal esterase of rat liver. J Biol Chem 244: 2269–2274.

Hosokawa M (2008). Structure and catalytic properties of carboxylesterase isozymes involved in metabolic activation of prodrugs. Molecules 13: 412–431.

Huang L, Zhu C, Sun Y, Xie G, Mackenzie GG, Qiao G *et al*. (2010). Phospho-sulindac (OXT-922) inhibits the growth of human colon cancer cell lines: a redox/polyamine-dependent effect. Carcinogenesis 31: 1982–1990.

Huang L, Mackenzie G, Ouyang N, Sun Y, Xie G, Johnson F *et al*. (2011). The novel phospho-non-steroidal anti-inflammatory drugs, OXT-328, MDC-22 and MDC-917, inhibit adjuvant-induced arthritis in rats. Br J Pharmacol 162: 1521–1533.

Kaimul AM, Nakamura H, Masutani H, Yodoi J (2007). Thioredoxin and thioredoxin-binding protein-2 in cancer and metabolic syndrome. Free Radic Biol Med 43: 861–868.

Kashfi K, Rigas B (2005). Is COX-2 a 'collateral' target in cancer prevention? Biochem Soc Trans 33: (Pt 4): 724–727.

Kirschning A, Ries M, Domann S, Martin W, Albrecht W, Arnold P *et al*. (1997). Synthesis and biological identification of the acyl glucuronide of the antiinflammatory drug ML-3000. Bioorg Med Chem Lett 7: 903–906.

Lamboursain L, St-Onge F, Jolicoeur M (2002). A lab-built respirometer for plant and animal cell culture. Biotechnol Prog 18: 1377–1386.

Lanas A, Ferrandez A (2009). NSAIDs and the colon. Curr Opin Gastroenterol 25: 44–49.

Leite S, Martins NM, Dorta DJ, Curti C, Uyemura SA, dos Santos AC (2006). Mitochondrial uncoupling by the sulindac metabolite, sulindac sulfide. Basic Clin Pharmacol Toxicol 99: 294–299.

Liu D, Zheng X, Tang Y, Zi J, Nan Y, Wang S *et al*. (2010). Metabolism of tanshinol borneol ester in rat and human liver microsomes. Drug Metab Dispos 38: 1464–1470.

Ljungquist A, Augustinsson KB (1971). Purification and properties of two carboxylesterases from rat-liver microsomes. Eur J Biochem 23: 303–313.

Mackenzie GG, Sun Y, Huang L, Xie G, Ouyang N, Gupta RC *et al*. (2010). Phospho-sulindac (OXT-328), a novel sulindac derivative, is safe and effective in colon cancer prevention in mice. Gastroenterology 139: 1320–1332.

Mackenzie GG, Ouyang N, Xie G, Vrankova K, Huang L, Sun Y *et al*. (2011). Phospho-sulindac (OXT-328) combined with difluoromethylornithine prevents colon cancer in a mouse xenograft model. Cancer Prev Res (Phila) 4: 1052–1060.

Mantovani A, Allavena P, Sica A, Balkwill F (2008). Cancer-related inflammation. Nature 454: 436–444.

Meyskens FL, McLaren CE, Pelot D, Fujikawa-Brooks S, Carpenter PM, Hawk E *et al*. (2008). Difluoromethylornithine plus sulindac for the prevention of sporadic colorectal adenomas: a randomized placebo-controlled, double-blind trial. Cancer Prev Res (Phila) 1: 9–11.

Morishita Y, Fujii M, Kasakura Y, Takayama T (2005). Effect of carboxylesterase inhibition on the anti-tumour effects of irinotecan. J Int Med Res 33: 84–89.

Nagy A, Plonowski A, Schally AV (2000). Stability of cytotoxic luteinizing hormone-releasing hormone conjugate (AN-152) containing doxorubicin 14-O-hemiglutarate in mouse and human serum *in vitro*: implications for the design of preclinical studies. Proc Natl Acad Sci U S A 97: 829–834.

Piazza GA, Keeton AB, Tinsley HN, Gary BD, Whitt JD, Mathew B *et al*. (2009). A novel sulindac derivative that does not inhibit cyclooxygenases but potently inhibits colon tumor cell growth and induces apoptosis with antitumor activity. Cancer Prev Res (Phila) 2: 572–580.

Ratnayake JH, Hanna PE, Anders MW, Duggan DE (1981). Sulfoxide reduction. *In vitro* reduction of sulindac by rat hepatic cytosolic enzymes. Drug Metab Dispos 9: 85–87.

Rigas B (2007). The use of nitric oxide-donating nonsteroidal anti-inflammatory drugs in the chemoprevention of colorectal neoplasia. Curr Opin Gastroenterol 23: 55–59.

Rigas B, Williams JL (2008). NO-donating NSAIDs and cancer: an overview with a note on whether NO is required for their action. Nitric Oxide 19: 199–204.

Roberts J II, Morrow J (2001). Analgesic-antipyretic and antiinflammatory agents and drugs employed in the treatment gout. In: Hardman JG, Limbird LE (eds). Goodman and Gilman's The Pharmacological Basis of Therapeutics, 10th edn. McGraw-Hill: New York, pp. 687–731.

Shiff SJ, Rigas B (1999). The role of cyclooxygenase inhibition in the antineoplastic effects of nonsteroidal antiinflammatory drugs (NSAIDs), [comment]. J Exp Med 190: 445–450.

Shiff SJ, Qiao L, Tsai LL, Rigas B (1995). Sulindac sulfide, an aspirin-like compound, inhibits proliferation, causes cell cycle quiescence, and induces apoptosis in HT-29 colon adenocarcinoma cells. J Clin Invest 96: 491–503.

Sostres C, Gargallo CJ, Arroyo MT, Lanas A (2010). Adverse effects of non-steroidal anti-inflammatory drugs (NSAIDs, aspirin and coxibs) on upper gastrointestinal tract. Best Pract Res Clin Gastroenterol 24: 121–132.

Steinbrink SD, Pergola C, Buhring U, George S, Metzner J, Fischer AS *et al*. (2010). Sulindac sulfide suppresses 5-lipoxygenase at clinically relevant concentrations. Cell Mol Life Sci 67: 797–806.

Taketani M, Shii M, Ohura K, Ninomiya S, Imai T (2007). Carboxylesterase in the liver and small intestine of experimental animals and human. Life Sci 81: 924–932.

Wallace JL (2008). Prostaglandins, NSAIDs, and gastric mucosal protection: why doesn't the stomach digest itself? Physiol Rev 88: 1547–1565.

Wallace JL, Vong L (2008). NSAID-induced gastrointestinal damage and the design of GI-sparing NSAIDs. Curr Opin Investig Drugs 9: 1151–1156.

Xie G, Sun Y, Nie T, Mackenzie GG, Huang L, Kopelovich L *et al*. (2011). Phospho-ibuprofen (MDC-917) is a novel agent against colon cancer: efficacy, metabolism, and pharmacokinetics in mouse models. J Pharmacol Exp Ther 337: 876–886.

Yarrington JT, Sprinkle DJ, Loudy DE, Diekema KA, McCann PP, Gibson JP (1983). Intestinal changes caused by DL-alpha-difluoromethylornithine (DFMO), an inhibitor of ornithine decarboxylase. Exp Mol Pathol 39: 300–316.

Supporting information

Additional Supporting Information may be found in the online version of this article:

Figure S1 Kinetics of PS and its metabolites by human intestinal microsomes. PS (60 μM) was incubated with human intestinal microsomes as described in the Methods section at 37°C for up to 90 min. PS and its metabolites were extracted and analysed by HPLC.
Figure S2 Hydrolysis of PS by esterase. PS (120 μM) was treated with porcine liver esterase (0.5 $mg \cdot mL^{-1}$) at 37°C for up to 90 min, and the drug levels were determined by HPLC.
Figure S3 Kinetics of PS sulphide in Trx-knockdown cells. PS (100 μM) was incubated with Trx-knockdown or control MDA-MB-231 cells at 37°C for up to 6 h. PS sulphide was extracted at the designated time points and analysed by HPLC.
Figure S4 Inhibition of the hydrolysis of PS in mouse plasma by BNPP. Mouse plasma was incubated with or without BNPP at 37°C for 30 min, and the resulting plasma was incubated with PS (400 μM) at 37°C for 10 min. The remaining drug levels were determined by HPLC. Presented as percentage of intact PS at indicated BNPP concentrations.
Figure S5 Identification of the SSone and SSide glucuronides. A: MS/MS spectrum of SSone glucuronide fraction collected from HPLC. B: MS/MS spectrum of SSide glucuronide fraction collected from HPLC.

Please note: Wiley-Blackwell are not responsible for the content or functionality of any supporting materials supplied by the authors. Any queries (other than missing material) should be directed to the corresponding author for the article.